Journal of Thermal Analysis and Calorimetry, Vol. 68 (2002) 1045–1059

STUDIES ON SOME TRANSITION METAL MIXED LIGANDS COMPLEXES
Glycinyldithiocarbamate and 8-hydroxyquinoline moiety

A. S. A. Zidan[*]

Chemistry Department, Faculty of Science, Assiut University, Assiut, Egypt

(Received June 28, 2001; in revised form January 3, 2002)

Abstract

This paper reports the isolation and characterisation of mixed ligand complexes of the types Ba[M(Ox)$_2$glydtc], [M$'_2$(Ox)$_4$glydtc], [M$_2$(QA)$_2$glydtc] and [M$'_2$(QA)$_4$glydtc] (where *glydtc*=glycinyldithiocarbamate; *HOx*=8-hydroxyqinoline; *HQA*=*p*-methyl-5-phenylazo-8-hydroxyquinoline and *M*=Co(II), Ni(II) or Cu(II); *M′*=Fe(III) or Cr(III). The structures for the complexes have been elucidated on the basis of elemental analysis, electronic, IR and mass spectroscopy. Electronic spectral data for the complexes were in accordance with an octahedral environment around the central metal ions in all metal chelates except for [Co$_2$(QA)$_2$glydtc] and [Ni$_2$(QA)$_2$glydtc] where the structure around Co(II) and Ni(II) may be tetrahedral. The complexes were proposed to be dimeric except those of Ba[M(Ox)$_2$glydtc]. A study of the thermal decomposition of the complexes has also been carried out. For Ba[M(Ox)$_2$glydtc], elimination of carbon dioxide was observed. However, evolution of nitrogen and formation of tolyl radicals occur for [M$_2$(QA)$_2$glydtc] and [M$'_2$(QA)$_4$glydtc]. Kinetic parameters for the various decomposition stages were calculated using the Coats–Redfern and Horowitz–Metzger equations.

Keywords: glycinyldithiocarbamate, 8-hydroxyquinoline moiety, mixed ligand complexes, spectral and thermal analysis

Introduction

Dithiolate metal complexes constitute a large family of compounds, which have been deeply investigated from several points of view [1–3]. In the most recent years, many studies have been developed on dithiocarbamate metal complexes in order to gain more information about the role of these complexes played in chemical industry, biology and biochemistry [4, 5]. The metal complexes of dithiocarbamates derived from α-aminoacids have been successfully used in agriculture for controlling insects and fungi as well [6].

---

[*] E-mail: amna@aun.eun.eg

1418–2874/2002/ $ 5.00

Akadémiai Kiadó, Budapest
Kluwer Academic Publishers, Dordrecht

Some of the 8-hydroxyquinoline derivatives and their complexes with transition metals were reported to be active against bacteria [7]. The 8-hydroxyquinoline azo compounds were involved in industry as polymerization inhibitors and as analytical reagents [8]. Their azo group involved in a number of biological carcinogenesis and nitrogen fixation [9].

In view of the above importance of dithiocarbamates amino acids, we have previously studied several complexes formed from these dithiocarbamates and acetylacetonate complex [10]. In this article we prepared and studied the mixed ligand complexes of Co(II), Ni(II), Cu(II), Fe(III) and Cr(III) containing the ligands, 8-hydroxyquinoline (HOx) or *p*-methyl-5-phenylazo-8-hydroxyquinoline (HQA) and glycinyldithiocarbamate (glydtc) $[S_2CNHCH_2COO]^{-2}$.

Experimental

Glycine and 8-hydroxyquinoline were purchased from BDH grade carbon disulphide provided by Prolabo. All other chemicals were of high purity and were used as purchased, without any further purification. The barium salt of glycinyldithiocarbamate, HQA and bis(8-hydroxyquinolinato)cobalt(II), nickel(II), and copper(II) were prepared according to the literature procedures [11, 12].

Physical measurements

The infrared spectra were recorded on a 470 Shimadzu infrared spectrophotometer as KBr pellet. The electronic absorption spectra measurements (in dimethylformamide solution) were carried out on an UV-2101 PC Shimadzu spectrophotometer. JEOL-JMS600 apparatus recorded the mass spectra. The thermogravimetric analyses were performed using an electrobalance of the type of Sartorius 200 MP converted to a thermobalance by the addition of a small furnace and sample holder. The temperature was measured using a Chromal-Alumal thermocouple attached to a digital multimeter type soar ME-550; the heating rate was adjusted to be 8°C $\min^{-1}$. The elemental analysis performed by an elemental vario EL Fab-No. 11982027 apparatus.

Preparation of the mixed ligand complexes

Barium bis(8-hydroxyquinolinato) (glycinyldithiocarbamato)nickel(II)

Because the preparative methods of the complexes for Co(II), Ni(II) or Cu(II) are similar, the preparation of barium bis(8-hydroxyquinolinato) (glycinyldithiocarbamato)nickel(II) is representative. An aqueous solution (20 mL) of 1 mmol barium glycinyldithiocarbamate was added with continuous stirring to warm ethanolic solution (20 mL) of 1 mmol bis(8-hydroxyquinolinato)nickel(II). The resulting solution was refluxed for 2 h. The product separated out on cooling; it was filtered, washed with a 1:1 mixture of absolute ethanol and water and dried over P_4O_{10} about four days.

For preparing Fe(III) and Cr(III) complexes

2 Mmol of 8-ydroxyquinoline or *p*-methyl-5-phenylazo-8-hydroxyquinoline in 25 mL hot ethanol (40–45°C) was added dropwise to 1 mmol of the metal chloride in 20 mL aqueous ethanolic solution with continuous stirring, binary complexes were formed. Upon the addition of 25 mL of 1 mmol barium glycinyldithiocarbamate solution the mixed ligand complexes were formed immediately. The mixture was stirred for about 1 h and refluxed for about 6 h. The products were filtered off, washed with a 1:1 mixture of absolute alcohol and water to remove any unreacted metal salt and ligands. All complexes were dried over P_4O_{10}.

Results and discussion

The elemental analysis data together with colour and decomposition points of the solid chelates are listed in Table 1.

Table 1 Colour, elemental analysis and melting point of the complexes

(No.) Complex	Colour	Found (calc.%) C	H	N	S	Dec. point/°C
(1) Ba[Co(Ox)$_2$glydtc]	pink	39.85 (39.80)	2.40 (2.39)	6.65 (6.63)	10.15 (10.12)	310
(2) Ba[Ni(Ox)$_2$glydtc]	green	39.75 (39.81)	2.40 (2.39)	6.65 (6.63)	10.16 (10.12)	325
(3) Ba[Cu(Ox)$_2$glydtc]	yellow	39.56 (39.51)	2.36 (2.37)	6.60 (6.58)	10.10 (10.05)	300
(4) [Fe$_2$(Ox)$_4$glydtc]	green	36.02 (55.93)	3.26 (3.25)	8.34 (8.36)	7.65 (7.66)	340
(5) [Cr$_2$(Ox)$_4$glydtc]	brown	56.53 (56.45)	3.30 (3.28)	8.40 (8.44)	7.70 (7.73)	280
(6) [Co$_2$(QA)$_2$glydtc]	brown	53.23 (53.41)	3.45 (3.44)	12.32 (12.39)	8.05 (8.10)	350
(7) [Ni$_2$(QA)$_2$glydtc]	orange	53.02 (53.13)	3.45 (3.44)	12.42 (12.39)	8.15 (8.11)	360
(8) [Cu$_2$(QA)$_2$glydtc]	dark green	52.38 (52.49)	3.42 (3.40)	12.32 (12.24)	8.09 (8.01)	365
(9) [Fe$_2$(QA)$_4$glydtc]	dark green	61.52 (61.43)	3.90 (3.92)	13.96 (13.90)	4.86 (4.90)	370
(10) [Cr$_2$(QA)$_4$glydtc]	brown	61.82 (61.79)	3.96 (3.95)	14.00 (13.98)	4.95 (4.92)	355

The general equations for the complexes are shown as follows:

$$\mathrm{M(Ox)_2{+}Baglydtc{\rightarrow}Ba[M(Ox)_2glydtc]} \quad (1)$$

$$\mathrm{2M'Cl_3{+}4HOx{+}Baglydtc{\rightarrow}[2M'_2(Ox)_4glydtc]{+}BaCl_2{+}4HCl} \quad (2)$$

$$\mathrm{2MCl_2{+}2HQA{+}Baglydtc{\rightarrow}[M_2(QA)_2glydtc]{+}BaCl_2{+}2HCl} \quad (3)$$

$$\mathrm{2M'Cl_3{+}4HQA{+}Baglydtc{\rightarrow}[2M'_2(QA)_4glydtc]{+}BaCl_2{+}4HCl} \quad (4)$$

where *M*=Co(II), Ni(II) or Cu(II); *M′*=Fe(III) or Cr(III); *Ox*=8-hydroxyquinolinate; *QA*=*p*-methyl-5-phenylazo-8-hydroxyquinolinate and *glydtc*=glycinyldithiocarbamate.

The mixed ligand complexes of 8-hydroxyquinoline-glydtc with Co(II), Ni(II) and Cu(II) are partially soluble in most organic solvents; hence, it was not possible to measure their molar conductivity.

IR spectra

The most significant bands of the IR spectra of the complexes are recorded in Table 2. Our data on the IR spectra of the complexes show the characteristic bands of dithiocarbamate, 8-hydroxyquinolinate or *p*-methyl-5-phenylazo-8-hydroxyquinolinate moieties.

A band appears in the range 3300–3400 cm^{-1}, which is assigned, to ν(N–H) stretching mode of the dithiocarbamate. For the CN groups, two bands are recorded, one at 1490–1510 cm^{-1} due to the $\mathrm{NCS_2^-}$ group and the other at 1090–1110 cm^{-1} due to the $\mathrm{NCCO_2^-}$ group (at 1505 and 1155 cm^{-1} for the ligand). This is in accordance with previously reported IR data on dithiocarbamate metal complexes [13].

The bands at 1420–1435 and 1566–1590 cm^{-1} in the spectra of the complexes may be assigned respectively, to ν_s(COO$^-$) and ν_{as}(COO$^-$) of the coordinated carboxylate group. These bands are shift about 25 and 15 cm^{-1} to higher wavelength if compared with those of the ligand (1410 and 1565 cm^{-1}). Moreover, the presence of two bands in the regions 990–1020 and 620–650 cm^{-1} in the IR spectra may be attributed to the stretching vibration of $\mathrm{CS_2}$ group of the dithiocarbamate moiety. For the dithiocarbamate ligand the later bands are observed at 1000 and 595 cm^{-1} respectively. The presence of two bands for $\mathrm{CS_2}$ group is previously reported for related complex [11].

Furthermore, the 8-hydroxyquinolinate and *p*-methyl-5-phenylazo-8-hydroxyquinolinate moieties display two bands in the regions 1120–1140 and 1575–1590 cm^{-1} corresponding to ν(C–O) and ν(C=N) respectively. Moreover, ν(N=N) was recorded at 1380–1400 cm^{-1} for azo complexes [14]. The position of ν(C=N) and ν(C–O) indicates that the coordination occurs through nitrogen and oxygen of 8-hyroxyquinolinate part for all the complexes. The M–N stretching frequency in some complexes is obtained at higher wave number (645–750 cm^{-1}) due to M→N π=interaction. Nakamato [15] has shown that M–N stretching frequency undergoes coupling with other stretching vibrations resulting in a number of bands. The bands around 780 and 640 cm^{-1} may correspond to the coupled M–N vibrations [16].

Table 2 IR absorption of the complexes (cm^{-1})

Complex	ν_s(N–H)	ν(NCCO$_2$)	ν(NCS$_2$)	ν_s(COO$^-$)	ν_{as}(COO$^-$)	ν_{as}(C–S)	ν_s(C–S)	ν(N=N)	ν(C=N)	ν(CO)	ν(M–N)
(1)	3350	1110	1490	1430	1570	1000	640	–	1590	1130	645, 740
(2)	3380	1110	1490	1420	1568	990	640	–	1580	1135	420, 650
(3)	3350	1105	1500	1435	1566	990	620	–	1585	1140	415, 645
(4)	3350	1100	1505	1420	1580	1010	630	–	1580	1120	420, 750
(5)	3350	1110	1510	1430	1590	1005	625	–	1590	1120	425, 750
(6)	3400	1090	1495	1420	1585	995	650	1380	1580	1130	420, 750
(7)	3300	1100	1490	1430	1587	1010	630	1400	1575	1140	430, 740
(8)	3400	1090	1505	1425	1580	990	650	1390	1580	1135	425, 745
(9)	3350	1090	1510	1430	1590	1020	625	1380	1585	1130	425, 740
(10)	3300	1090	1510	1420	1587	1020	640	1390	1580	1140	730, 750

Electronic spectra

The principal bands of the visible and UV-spectra of the complexes are given in Table 3. The electronic spectra for all ternary complexes in formulae Ba[M(Ox)$_2$glydtc] and [M$'_2$(Ox)$_4$glydtc] exhibit *d–d* bands characteristic of an octahedral geometry around the metal ion. For the spectra of the complexes which in the formula Ba[M(Ox)$_2$glydtc], the Co(II) complex display a *d–d* band at 16.186 cm^{-1} attributed to $^4A_{2g}\rightarrow{}^4T_{1g}(P)$ transition, that of the Ni(II) complex is in two bands at 15.148 and 25.381 cm^{-1} which may be assigned to $^3A_{2g}\rightarrow{}^3T_{1g}(F)$ and $^3A_{2g}\rightarrow{}^3T_{1g}(P)$ transitions respectively [17]. For the Cu(II) complex the *d–d* bands is observed at 15.152 cm^{-1} ($^2B_{1g}\rightarrow{}^2A_{1g}$ ν_1 transition).

Table 3 Electronic spectral data of the complexes (cm^{-1})

Complex	*d–d*	Intraligand transition
Ba[Co(Ox)$_2$glydtc]	16.186 24.601	37.736
Ba[Ni(Ox)$_2$glydtc]	15.148 25.381	38.418
Ba[Cu(Ox)$_2$glydtc]	15.152	24.038, 37.175, 45.045
[Fe$_2$(Ox)$_4$glydtc]	17.736 23.866	30.240, 37.594, 44.052
[Cr$_2$(Ox)$_4$glydtc]	17.065 23.866	30.960, 36.765, 43.103
[Co$_2$(QA)$_2$glydtc]	20.964 (CT)	28.902, 32.258, 39.063, 46.083
[Ni$_2$(QA)$_2$glydtc]	21.367 (CT)	37.879
[Cu$_2$(QA)$_2$glydtc]	12.136 20.243 (CT)	27.248, 37.453
[Fe$_2$(QA)$_4$glydtc]	17.271 21.271	26.954, 40.650
[Cr$_2$(QA)$_4$glydtc]	17.321 23.241	30.026, 38.568

CT=charge transfer

The two complexes [Fe$_2$(Ox)$_4$glydtc] and [Cr$_2$(Ox)$_4$glydtc] display two bands assigned to *d–d* transitions. Fe(III) complex exhibits two bands at 17.736 and 23.866 cm^{-1}, which are assigned to $^6A_{1g}\rightarrow{}^4T_{1g}(G)$ and $^6A_{1g}\rightarrow{}^4T_{2g}(G)$ transitions for an octahedral geometry, respectively. The Cr(III) complex gives two bands at 17.065 and 23.866 cm^{-1} which are assigned to $^4A_{2g}(F)\rightarrow{}^4T_{2g}(F)$ and $^4A_{2g}(F)\rightarrow{}^4T_{1g}(F)$ transitions respectively for an octahedral structure [18].

For the complexes [M$_2$(QA)$_2$glydtc] and [M$'_2$(QA)$_4$glydtc], an intense band is observed in the range 20.243–21.367 cm^{-1} which may be attributed to the characteristic azo $n\rightarrow\pi^*$ [17]. The *d–d* transition bands for both the complexes [Co$_2$(QA)$_2$glydtc] and [$Ni_2(QA)_2$glydtc] is masked by the azo group absorption band in this region. The close similarity between the electronic spectra of the complexes and related compounds (e.g. transition metal complexes of azo-8-hydroxyquinoline derivatives [19]) indicates the tetrahedral structure around Co(II) and Ni(II). The Cu(II) complex shows a *d–d* band at 12.136 cm^{-1} which is assigned to $^2B_{1g}\to{}^2A_{1g}(\nu_1)$ transition for an octahedral structure. The six coordination geometry around Cu(II) may be attained through molecular association in the latter complex. The *d–d* transitions of Fe(III) and Cr(III) complexes of the type [$M'_2(QA)_4$glydtc] occur at almost the same positions as in the complexes [$M'_2(Ox)_4$glydtc]. This means that these complexes may have an octahedral structure.

Finally, most of the ternary complexes exhibit three types of intraligand transition in the ranges 26.595–30.959; 32.258–38.641 and 40.322–43.668 cm^{-1}, which may be assigned to $n\to\pi^*$ (dtc) [20], π–π^* between within the $S\overset{\cdots}{-}C\overset{\cdots}{-}S$ moiety [13] and the third is attributed to π–π^* transition within the molecular orbital originated in $N\overset{\cdots}{-}C\overset{\cdots}{-}S$ moiety [6].

Based on the above results, an octahedral structure is proposed to all metal ion complexes except a tetrahedral structure was proposed for Co(II) and Ni(II) ions with *p*-methyl-5-phenylazo-8-hydroxyquinolinate and glycinyldithiocarbamate complexes. The suggested structures of the complexes can be represented by

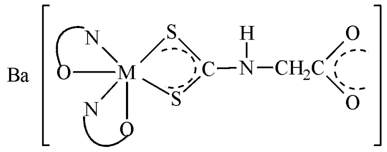

M=Co(II), Ni(II) or Cu(II)

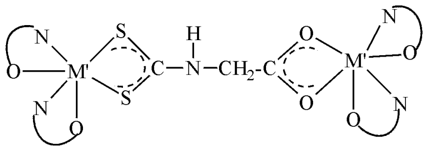

N O = 8-hydroxyquinolinate or *p*-methyl-5-phenylazo-8-hydroxyquinolinate anion

M=Co(II) or Ni(II)

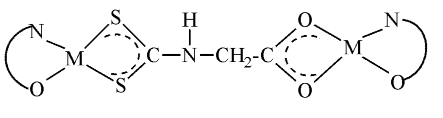

N O = *p*-methyl-5-phenylazo-8-hydroxyquinolate anion

M′=Fe(III) or Cr(III)

Thermal studies

The thermogravimetric analysis of the complexes was recorded in the 50–600°C range. TG and DTG curves of Ba[Co(Ox)$_2$glydtc] (Fig. 1) and Ba[Ni(Ox)$_2$glydtc] (Fig. 2) consist of three decomposition steps at 137, 270, 410°C and 155, 380, 450°C respectively. TG curve of Ba[Cu(Ox)$_2$glydtc] exhibits only two steps at 150 and 310°C. The first step of each of the above decomposition curve corresponds to the elimination of a carbon dioxide molecule from glycinyldithiocarbamate moiety. The decomposition can be represented by this equation:

$$\mathrm{Ba[M(Ox)_2S_2CNHCH_2CO_2]} \xrightarrow{-\mathrm{CO_2}} \mathrm{Ba[M(Ox)_2S_2CNHCH_2]} \quad (5)$$

where *M*=Co(II), Ni(II) or Cu(II).

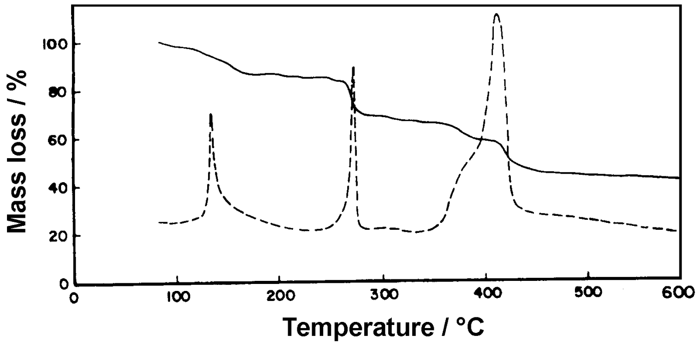

Fig. 1 TG and DTG curves of Ba[Co(Ox)$_2$glydtc]

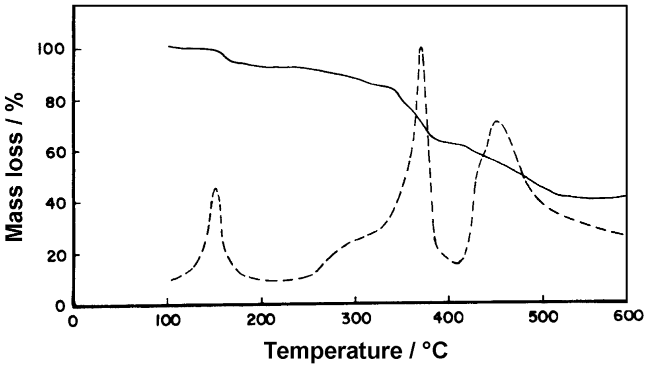

Fig. 2 TG and DTG curves of Ba[Ni(Ox)$_2$glydtc]

Decarboxylation was observed upon thermal decomposition of palladium complexes of dithiocarbamates derived from α-amino acids [20]. The rest of the molecule decomposes in subsequent steps leading to the formation of metal and barium sulphides as final residue (from TG curve) (calc. 41.1, 41.1 and 40.8%; found 41.9, 42.0 and 41.0% respectively for Co(II), Ni(II) and Cu(II) complexes).

$[Fe_2(Ox)_4glydtc]$ and $[Cr_2(Ox)_4glydtc]$ complexes show two steps in the pyrolysis curves at 330, 452°C and 180, 410°C respectively. It was difficult to correlate the first step with the proper decomposition products for the two complexes, because this step is large extending from 270–400°C in iron(III) complex and from 150–200°C in chromium(III) complex and thus includes various products. However, the second step in both compounds at 452 and 410°C (DTG curve) respectively forms a corresponding carbonate, which decomposes to the final product metal oxides (from TG and IR bands at 560 and 620 cm^{-1}) (calc. 19.1 and 18.3%; found 18.7 and 18.0% respectively).

The complexes $[Co_2(QA)_2glydtc]$ and $[Ni_2(QA)_2glydtc]$ show the same decomposition pattern; they decompose in two steps at 135, 350°C and 150, 420°C respectively. The first step is related to the evolution of two nitrogen molecules (calc. 7.1%, found 6.8 and 7.2% respectively) giving compound(I) which decomposed in the second step to give the final product; it may be CoO and NiO respectively. Elimination of nitrogen molecule from metal complexes of 5-aryl-azo-8-hydroxyquinoline during their thermal decomposition is known in literature [14].

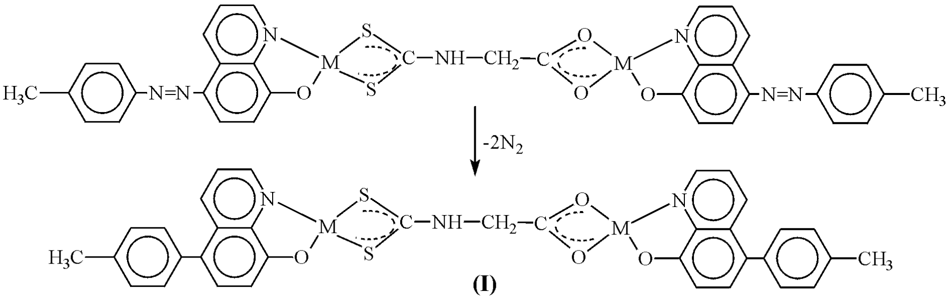

(I)

M=Co(II) or Ni(II)

$[Cu_2(QA)_2glydtc]$ (Fig. 3) shows three decomposition steps at 128, 270 and 435°C. The first step indicates the expulsion of two nitrogen molecules (calc. 6.9%, found 7.2%). The second step represents 28.5% loss corresponding to one molecule of carbon dioxide and two 4-methylphenil free radicals.

Dimerization of 4-methylphenyl radical may occur to give the product 4,4'-dimethylbiphenyl molecule (calc. 28.2%, found 28.5%) forming unstable complex. The rest of the molecule decomposes in the third step to form CuO (calc.19.8; found 20.0%).

A good correlation exists between the calculated and found values for $[Fe_2(QA)_4glydtc]$ compound. The first TG step at 250°C corresponds to the removal of four nitrogen molecules (calc. 8.6%, found 8.9%). The evolution of nitrogen molecule from azo compounds was recorded in literature [10]. At 370°C, a second step was observed, which agrees with the theoretical mass loss of the decarboxylation and four tolyl radicals, which may dimerize to form two molecules from 4,4' dimethylbiphenyl (calc. 31.1%, found 31.0%), thus leading to unstable compound which decomposes in the third step forming Fe_2O_3 as the end product (calc. 12.2, found 12.5%).

Kinetic data of the complexes

The kinetic data of each decomposition step is evaluated using the Coats–Redfern and Horowitz–Metzger methods [21, 22].

The Coats–Redfern equation

$$\ln\left[\frac{1-(1-\alpha)^{1-n}}{(1-n)T^2}\right]=M/T+B \quad \text{for } n\neq 1 \tag{6}$$

$$\ln\left[\frac{-\ln(1-\alpha)}{T^2}\right]=M/T+B \quad \text{for } n=1 \tag{7}$$

where α – fraction decomposed; T – absolute temperature and $M=-E/R$ and $B=\ln ZR/\phi E$; E, R, Z and ϕ are the activation energy, gas constant, pre-exponential factor and heating rate, respectively.

The Horowitz–Metzger equation

$$\ln\left[\frac{1-(1-\alpha)^{1-n}}{1-n}\right]=\ln\frac{ZRT_S^2}{\phi E}-\frac{E}{RT_S}+\frac{E\theta}{RT_S^2} \quad \text{for } n\neq 1 \tag{8}$$

$$\ln[-\ln(1-\alpha)]=\frac{E\theta}{RT_S^2} \quad \text{for } n=1 \tag{9}$$

where $\theta=T-T_S$; T_S is the temperature at the DTG peak.

The correlation coefficient r is computed using the least squares method for Eqs (6)–(9). Linear curves were drawn for different values of n ranging from 0 to 2, in in-

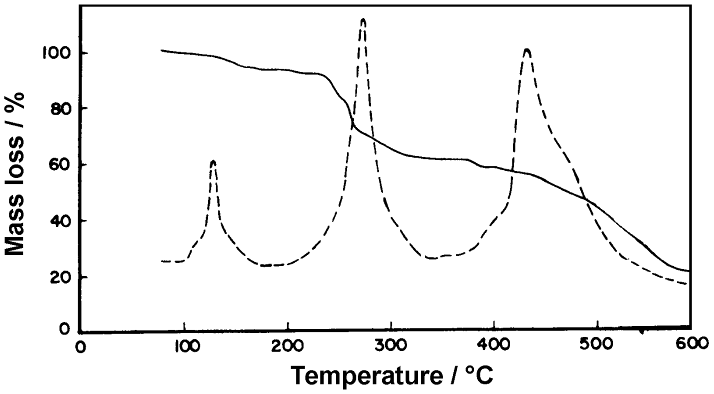

Fig. 3 TG and DTG curves of $[Cu_2(QA)_2glydtc]$

crements of 0.2. The value of n, which gave the best fit, was chosen as the order parameter for the decomposition stage of interest. The kinetic parameters were calculated from the plots of the left-hand side of Eqs (6) and (7) *vs.* $1/T$ and *vs.* θ for Eqs (8) and (9) (Figs 4 and 5).

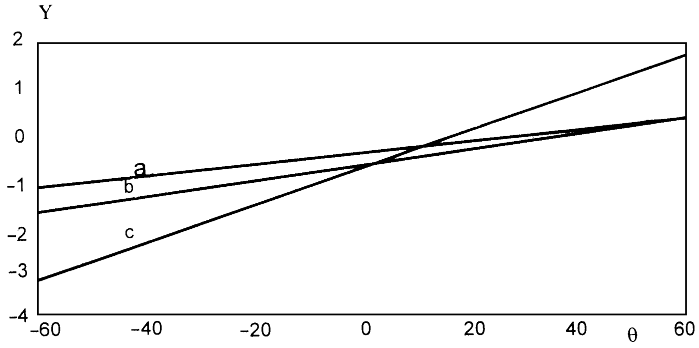

Fig. 4 Horowitz–Metzger plots for the three decomposition steps of [$Fe_2(QA)_4$glydtc] a – 1st step, b – 2nd step, c – 3rd step; where $y=\ln[1-(1-\alpha)^{1-n}T^{2}/(1-n)]$ for $n\neq1$ or $y=\ln[-\ln(1-\alpha)]$ for $n=1$

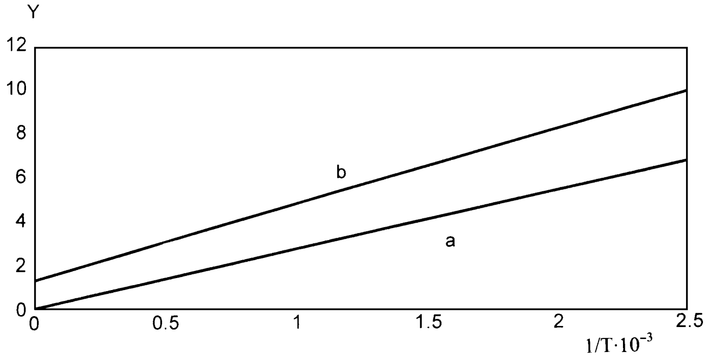

Fig. 5 Coats–Redfern plots for the two decomposition steps of Ba[$Ni(Ox)_2$glydtc] a – 1st step, b – 2nd step; where $y=\ln[1-(1-\alpha)^{1-n}/(1-n)T^2]$ for $n\neq1$ or $y=\ln[-\ln(1-\alpha)/T^2]$ for $n=1$

For all the complexes, the activation energy of the decomposition steps is recorded in Table 4. The activation energy for the decarboxylation in the first step of the complexes Ba[$Co(Ox)_2$glydtc], Ba[$Ni(Ox)_2$glydtc] and Ba[$Cu(Ox)_2$glydtc] lies in the range 50–77 kJ mol^{-1}. The activation energy of the first step for the complexes [$Fe_2(Ox)_4$glydtc] and [$Cr_2(Ox)_4$glydtc] are 71.7 and 49.6 kJ mol^{-1} respectively, indicating that the Fe(III) compound is more stable than the Cr(III) complex. Moreover, the complexes [$M_2(QA)_2$glydtc] and [$M'_2(QA)_4$glydtc] have an activation energy for the first step in the range 46.0–80.1 kJ mol^{-1}, which corresponds to the elimination of nitrogen molecule of the azo group in these complexes [17].

Table 4 Kinetic parameters of the thermal decomposition of the complexes

Complex	Step	Coats–Redfern			Horowitz–Metzger		
		n	*r*	E/kJ mol^{-1}	*n*	*r*	E/kJ mol^{-1}
$Ba[Co(Ox)_2glydtc]$	1st	1.00	0.9987	50	1.00	0.9970	51.5
	2nd	2.00	0.9970	185	2.00	0.9982	186
$Ba[Ni(Ox)_2glydtc]$	1st	0.66	0.9993	74.2	0.66	0.9910	77
	2nd	2.0	1.000	207.3	2.0	0.990	210
$Ba[Cu(Ox)_2glydtc]$	1st	1.00	0.9976	52.8	1.00	0.9960	54.6
	2nd	0.00	0.9900	104.6	0.00	1.000	106.8
$[Fe_2(Ox)_4glydtc]$	1st	1.00	0.9988	71.7	1.00	0.9990	73.5
	2nd	0.66	0.9950	109	0.66	1.000	112
$[Cr_2(Ox)_4glydtc]$	1st	0.00	0.9960	49.6	0.00	0.9990	52.4
	2nd	0.66	0.9980	98	0.66	1.000	100
$[Co_2(QA)_2glydtc]$	1st	2.00	0.9990	53.2	2	0.998	55.1
	2nd	0.00	0.9900	76.8	0	0.997	78.2
$[Ni_2(QA)_2glydtc]$	1st	0.33	0.9990	87.9	0.33	0.998	80.1
	2nd	2.00	0.9690	123.6	2.00	0.597	124.7
$[Cu_2(QA)_2glydtc]$	1st	2.00	0.9999	51.7	2.00	0.9978	52.9
	2nd	2.00	0.9900	152.2	2.00	1.000	156.7
	3rd	2.00	0.9980	199.7	2.00	0.9970	203.6
$[Fe_2(QA)_4glydtc]$	1st	1.0	0.9980	43.7	1.00	0.9920	46
	2nd	2.0	0.9990	70.4	2.00	0.9980	73.5
	3rd	0.66	0.9999	145.8	0.66	0.9990	197

Masss spectrometry

The mass spectral fragmentation pattern of $[Fe_2 (QA)_4glydtc]$ is depicted in Scheme 1 and the assignment is done on the basis of the most common ions, which reported in literature [20, 23] for similar compounds. One branch (a) of this scheme represents a series of fragments, corresponding to fragmentation of dithiocarbamate ligand [20], that loses a sulfur atom forming the species $[SCNHCH_2COO]^+$ m/z=117. This ion represents the base peak indicating its higher stability. Finally, the fragment ion $[N–C–CH_3]^+$ with m/z=41 is formed. The other branch (b) includes an iron-containing ligand fragment ion $[FeC_{32}H_{24}N_6O_2]^+$ of m/z=580, which loses two nitrogen molecules leading to the formation of $[FeC_{32}H_{24}N_2O_2]^+$ with m/z=524, and finally the fragment ion $[C_9H_6NO]^+$ with m/z=144 is formed [14].

It is to be noted that nitrogen molecules and tolyl radicals, which were assumed for the TG steps, are also detected in the mass spectrum of this iron complex at m/z=91.

Microbiological screening

The biological activities of some complexes were tested against a number of bacteria and fungi. The used bacteria were *P. aeruginosa* G-ve and *E. coli* G-ve while the

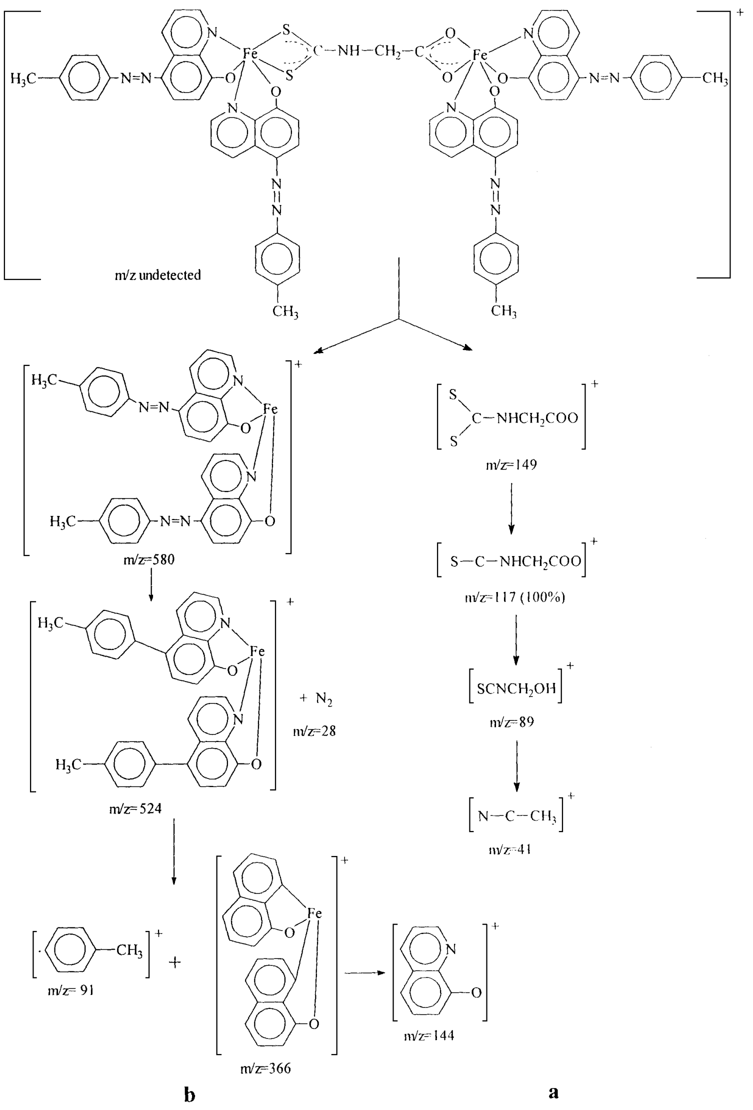

Scheme 1

tested fungi were *A. niger* and *Penicillium*. The culture media were nutrient agar (N.A) supplemented with one gm yeast /liter. The antibacterial and antifungal activity of each compound were evaluated by the classical filter paper technique The recorded data in Table 5 indicate that the complexes of 8-hydroxyquinolate anion and glycinyldithiocarbamate have the same activity on the bacteria and fungi. On the other hand, Fe(III) complex is more active than Co(II) complex for the same ligands.

Table 5 Microbiological screening

Complex	Bacteria		Fungi	
	P. Aeruginosa G-ve	*E. coli G-ve*	*A. niger*	*Penicillium*
Ba[Cu(Ox)$_2$]glydtc	++	+	+	+
[Fe$_2$(Ox)$_4$glydtc]	++	+	+	+
[Co$_2$(QA)$_2$glydtc]	+	++	++	+
[Fe$_2$(QA)$_4$glydtc]	+++	+++	+++	++

It is suggested that the neutral mixed ligand complexes penetrate the cell and at the site active may undergo dissociation into the corresponding 1:1 binary complexes as shown below:

$$[Fe_2(QA)_4glydtc] \leftrightarrow Fe(QA)_2^+ + Fe(glydtc)^+ + 2QA^- \qquad (10)$$

Thus, in the mixed-ligand complexes, the two binary complexes, $Fe(QA)_2^+$ and $Fe(glydtc)^+$, act as toxic agents and the resulting activity is a combination of both. Furthermore, the complexes may cause disturbance in the respiration process, thus blocking the synthesis of essential components of the cell [24].

Conclusions

The thermoanalytical results of the complexes Ba[M(Ox)$_2$glydtc] (where M=Co(II), Ni(II) or Cu(II)) prove that the main feature the first decomposition step is the evolution of carbon dioxide. The final products are metal and barium sulphides. Moreover, the evolution of nitrogen molecules and elimination of tolyl radical during the thermal analysis are related to some decomposition steps of the complexes, [M$_2$(QA)$_2$glydtc] and [M$'_2$(QA)$_4$glydtc]. The metal oxides were found as end products.

References

1 S. A. Gauveia, M. M. C. Nobrega and T. M. F. Severo, J. Therm. Anal. Cal., 59 (2000) 633.
2 Z. Lus, S. Chen, Y. Yu, J. Sun and S. J. Xiang, J. Therm. Anal. Cal., 55 (1999) 197.
3 R. J. Hilton, F. Oliveira, S. Espinola, J. Geraldo and G. Souza, Thermochim. Acta, 328 (1999) 187.
4 R. Liu, H. Tang and B. Zhang, Toxic. & Env. Chem., (1998).
5 A. F. M. El-Walily, O. A. Razak, S. F. Belal and R. S. Bakry, J. Pharm. & Biomedical Anal., 21 (1999) 439.
6 A. I. El-Said, A. S. A. Zidan, M. S. El-Meligy, A. A. M. Aly and O. F. Mohammed, Transition Met. Chem., 26 (2001) 13.
7 A. K. Patel and V. M. Patel, Synth. React. Inorg. Met-Org. Chem., 29 (1999) 193.
8 K. A. Khan, S. A. Kan, S. M. Khalid and A. A. Siddiqui, Arz. For., 44 (1994) 972.
9 C. E. Cerniglia, J. P. Freeman, W. Franklin and L. D. Pack, Carcinogenesis (London), 3 (1982) 1255.

10 A. S. A. Zidan, A. I. El-Said and A. A. Aly, Synth. React. Inorg. Met.-Org. Chem., 22 (1992) 1355.
11 M. Castillo, J. J. Griado, B. Macias and M. V. Vaquero, Inorg. Chim. Acta, 124 (1986) 127.
12 S. Takamoto, Q. Fernando and H. Freiser, Analyt. Chem., 37 (1965) 1249.
13 J. J. Criado, J. A. Lopez-Arias, B. Macias, L. R. Fernandez-Lago and J. M. Salas, Inorg. Chim. Acta, 193 (1992) 229.
14 A. S. A. Zidan, Synth. React. Inorg. Met.-Org. Chem., 24 (1994) 277.
15 K. Nakamoto, Infrared and Raman Spectra of Inorganic and Co-ordination Compounds, 4th ed., John Wiley Sons, 1993.
16 A. K. Patel, V. M. Patel, R. A. Patel, S. Sharma, J. J. Vora and J. D. Joshi, Synth. React. Inorg. Met.-Org. Chem., 29 (1999) 193.
17 A. S. A. Zidan, A. I. El-Said, M. S. El-Meligy, A. A. M. Aly and O. F. Mohammed, J. Therm. Anal. Cal., 62 (2000) 665.
18 B. B. Kaul and K. B. Pandeya, J. Inorg. Nucl. Chem., 40 (1978) 1035.
19 I. M. A. Awad, A. A. M. Aly, A. A. Abdel Hafez and K. H. M. Hassan, J. Chinese Chem. Soc., 36 (1989) 170.
20 J. J. Criado, I. Fernandez and B. Macias, Inorg. Chim. Acta, 174 (1990) 67.
21 A. W. Coats and J. P. Redfern, Nature, 20 (1964) 665.
22 H. H. Horowitz and G. Metzger, Anal. Chem., 35 (1963) 1464.
23 T. Tetsumi, M. Sumi, M. Tanka and T. Shono, 5 (1986) 706.
24 Y. Anjaneyulu and R. P. Rao, Synth. React. Inorg. Met.-Org. Chem., 16 (1986) 257.